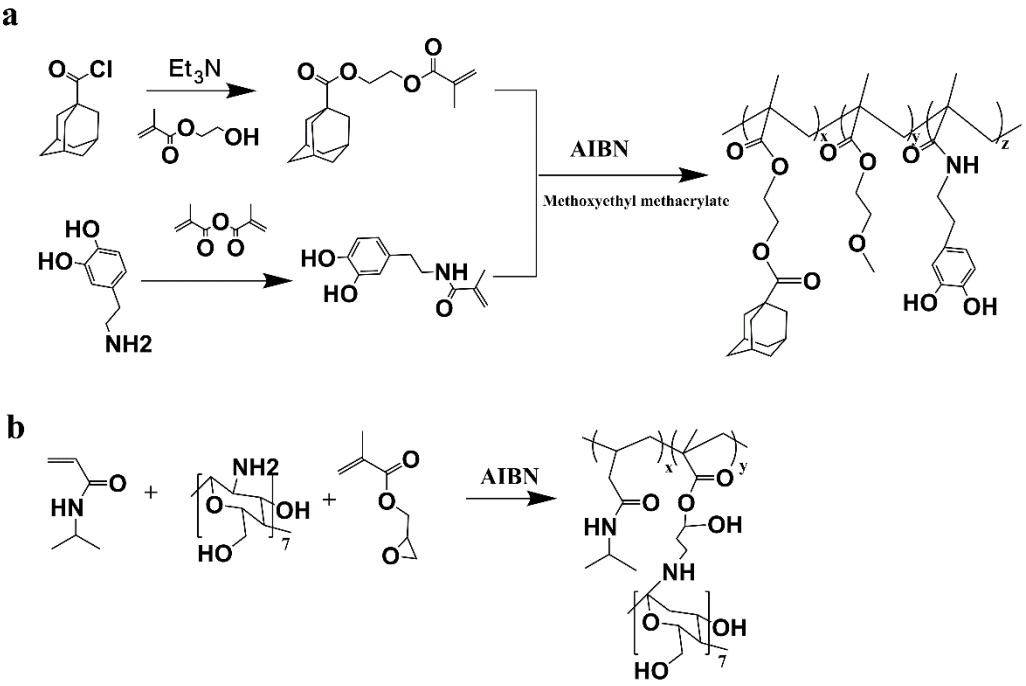


**Supplementary Figure 1 | Synthetic scheme of the guest and host copolymers**. **(a)** Guest copolymer pDOPA-AD-MEA is synthesized via free radical polymerization of AD monomer, DOPA monomer, and MEA. (**b**) Preparation of host copolymer pNIPAM-CD by the copolymerization of NIPAM and CD.

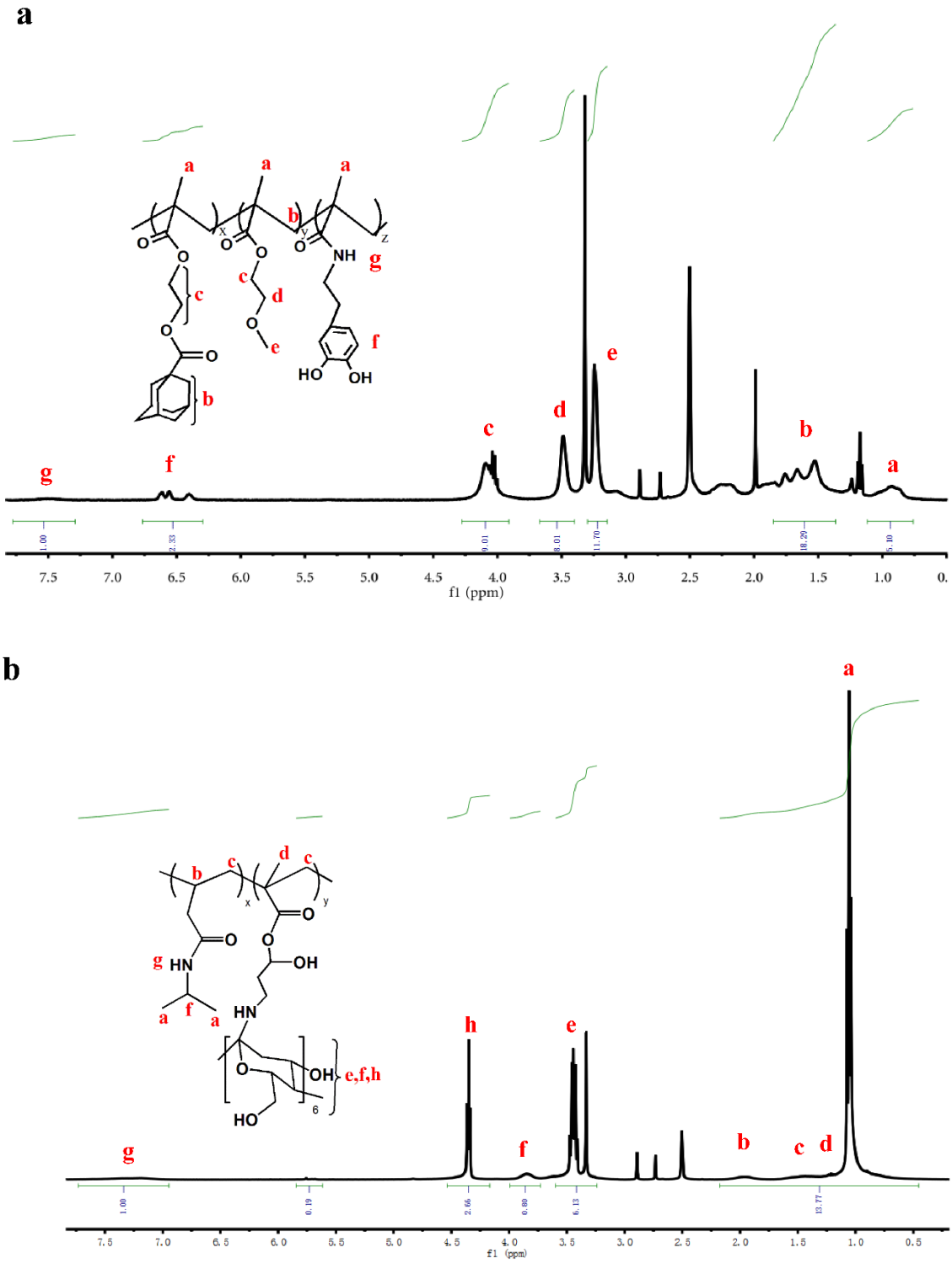


**Supplementary Figure 2 | The $^{1}$H NMR spectrum of the guest copolymer pDOPA-AD-MEA (a) and host copolymer pNIPAM-CD (b) in DMSO.** The characteristic NMR peaks corresponding to pDOPA-AD-MEA and pNIPAM-CD are clearly labeled.

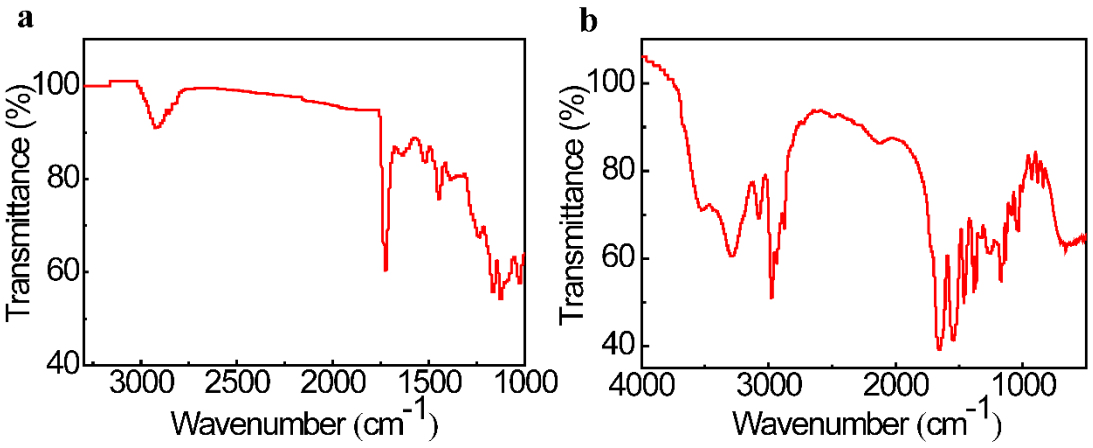


**Supplementary Figure 3 | FTIR spectra of the guest copolymer pDOPA-AD-MEA (a) and host copolymer pNIPAM-CD (b)**. (**a**) The characteristic peaks corresponding to the phenolic hydroxyl group (3430 $cm^{-1}$), ester acyl group (1730 $cm^{-1}$), and benzene group (1640) are clearly illustrated, suggesting the successful synthesis of the pDOPA-AD-MEA. (**b**) The characteristic peaks at 3290 $cm^{-1}$, 2970 $cm^{-1}$, 1660 $cm^{-1}$, and 1560 $cm^{-1}$ are assigned to the cyclodextrin hydroxyl group, methyl-methylene group, carbonyl group, and imino group, respectively, demonstrating the successful fabrication of the pNIPAM-CD.

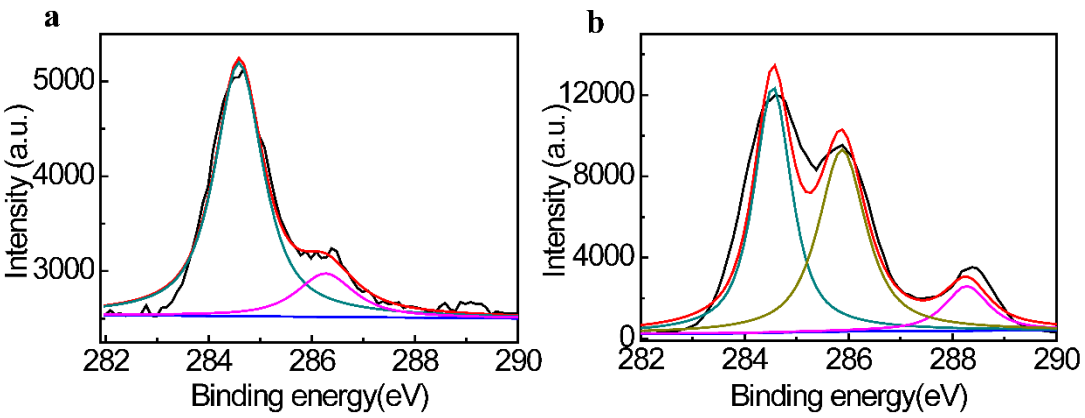


**Supplementary Figure 4 | High-resolution C1s XPS spectrum analysis of host copolymer and the adhesive coating.** (**a**) The characteristic peaks at 284.8 eV and 286.3 eV observed in the XPS spectrum are assigned to the C1s absorption of the ether group in pDOPA-AD-MEA. (**b**) After assembly of the host copolymer, an additional C1s absorption peak at 288.3 eV emerges, which corresponds to the carbonyl amide group in pNIPAM-CD.

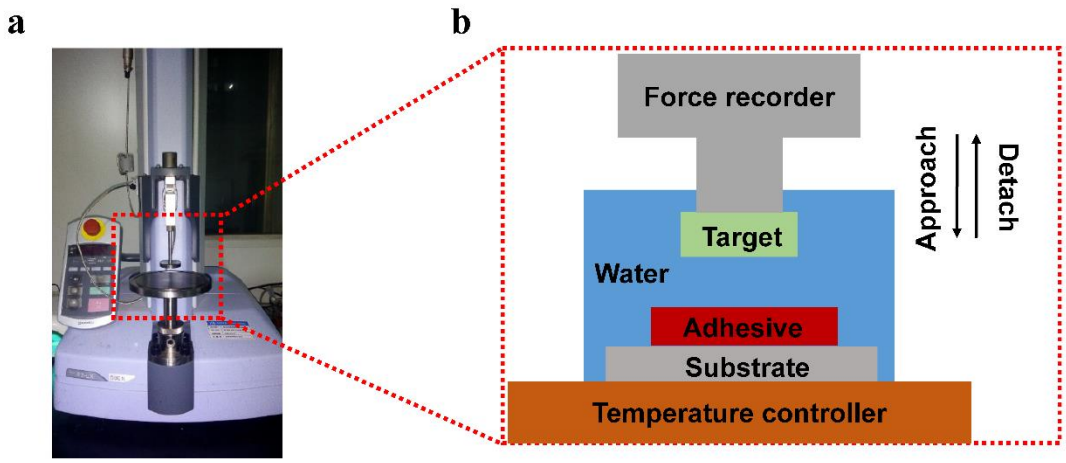


**Supplementary Figure 5 | Optical image of the UTM setup for the measurement of the interfacial adhesion**. (**a**) Optical photograph of UTM. (**b**) Schematic drawing showing the detailed set-up to characterize the interfacial adhesion.

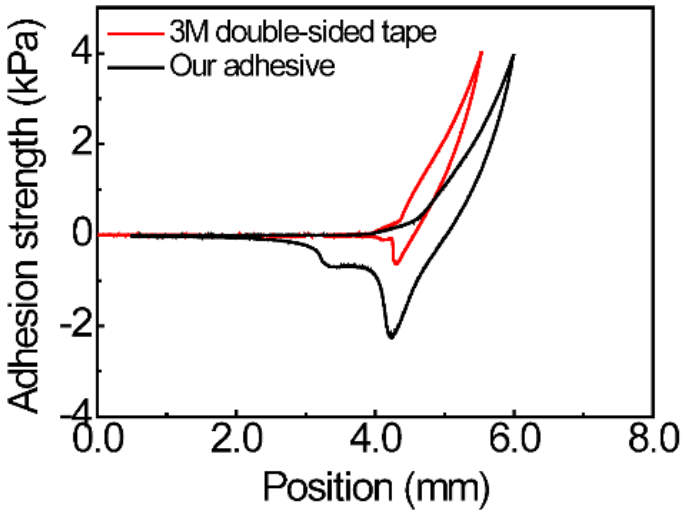


**Supplementary Figure 6 | Comparison of adhesion performances of adhesive coating and 3M double-sided tape**. In the wet environment, the adhesion strength of our adhesive is 5 times stronger than that of commercially available 3M double-sided tape.

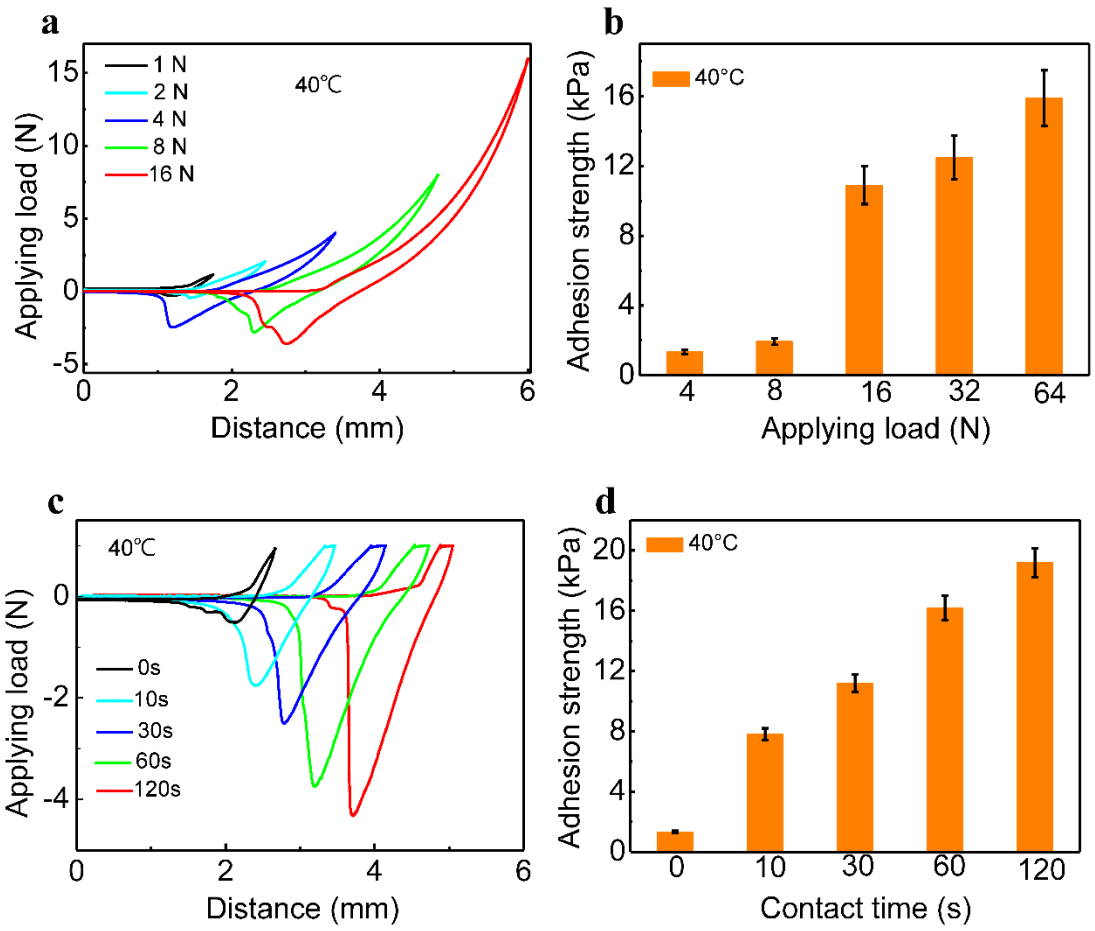


**Supplementary Figure 7 | Tailoring underwater adhesion by tuning pre-applying load and contact time.** (**a, b**) The variation of the adhesion properties under different applying loads. Here the contact time is maintained at 0 s and the temperature is 40 $^{o}$C. (**c, d**) The variation of the adhesion properties under different contact times. Here the applying load is maintained at 1 N and the temperature is 40 $^{o}$C. For an applying load of 1 N and contact time of 120 s, the adhesion strength is increased to 18 kPa.

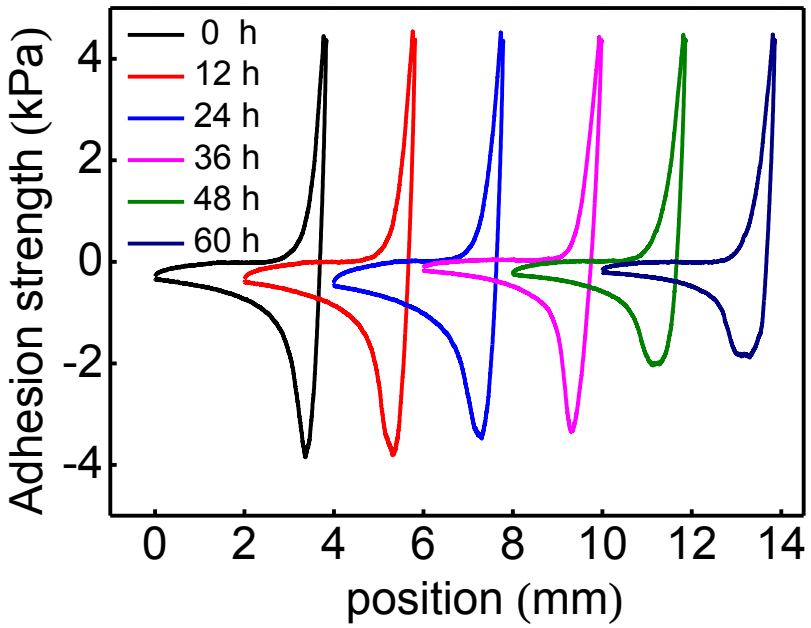


**Supplementary Figure 8 | Time-dependent variation of the adhesion strength at 40°C.** The adhesion strength of the adhesive coating is quite stable in the first 36 h and up to a continuous operation of 48 h, there is a marked drop in the adhesion strength.

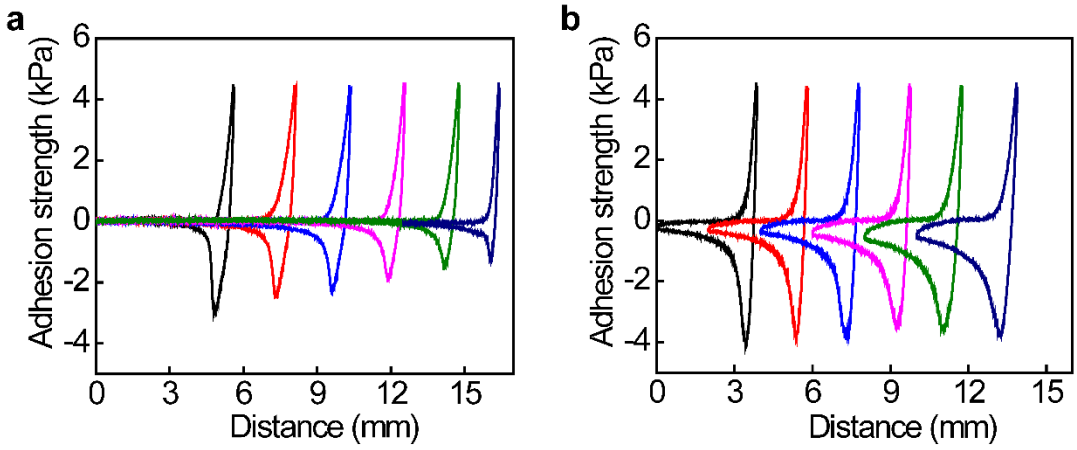


**Supplementary Figure 9 | Comparison of wet adhesion strength between control sample (AD-MEA-coated substrate) and AD-MEA-DOPA coated substrate at 40ºC**. (**a**) For the control sample, the adhesion strength exhibits a significant decay during successive tests. The curves in black, red, blue, pink, green and navy blue correspond to the tests conducted on 1$^{st}$, 11$^{th}$, 21$^{st}$, 31$^{st}$, 41$^{st}$, and 51$^{st}$ cycle, respectively. (**b**) For the wet adhesive made of AD-MEA-DOPA, there is no marked decay in the adhesion strength even after 50 cycles of tests.

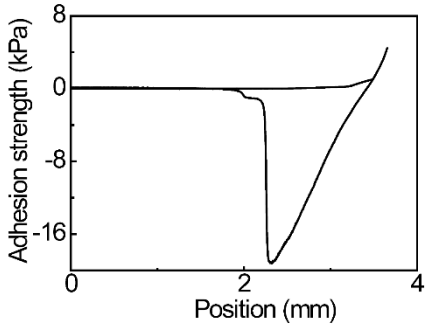


**Supplementary Figure 10| Adhesion strength of the adhesive coating in the air**. The adhesion strength of the adhesive coating at 25$^{o}$C and 40$^{o}$C in air is ~20 kPa, demonstrating that the thermo-reversible adhesion cannot be achieved in dry condition.

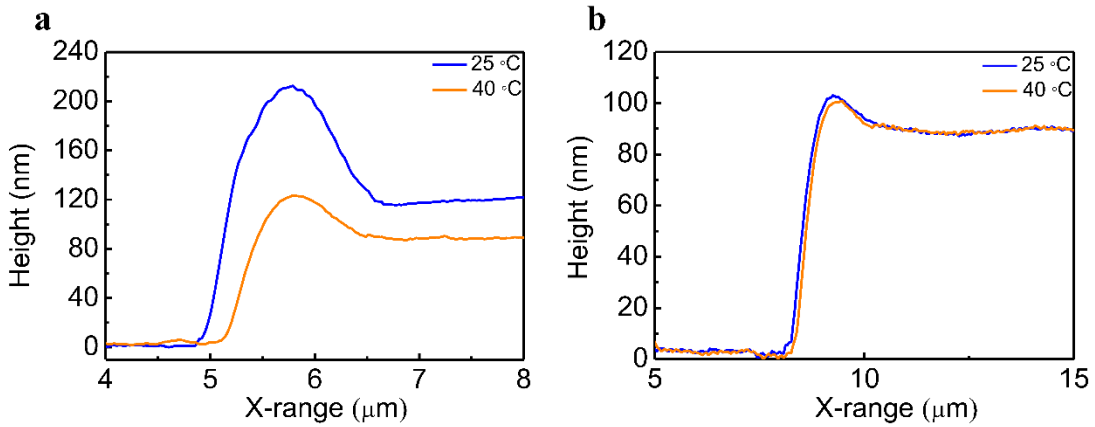


**Supplementary Figure 11 | Thickness measurement of the adhesive coating in wet and dry state**. (a) In the wet environment, the thickness of the adhesive coating at 25 $^{o}$C is 115 nm, which is larger than that at 40 $^{o}$C (90 nm). (b) In the dry environment, the thickness of the adhesive coating at 25 $^{o}$C is 80 nm, which is almost the same as that at 40 $^{o}$C.

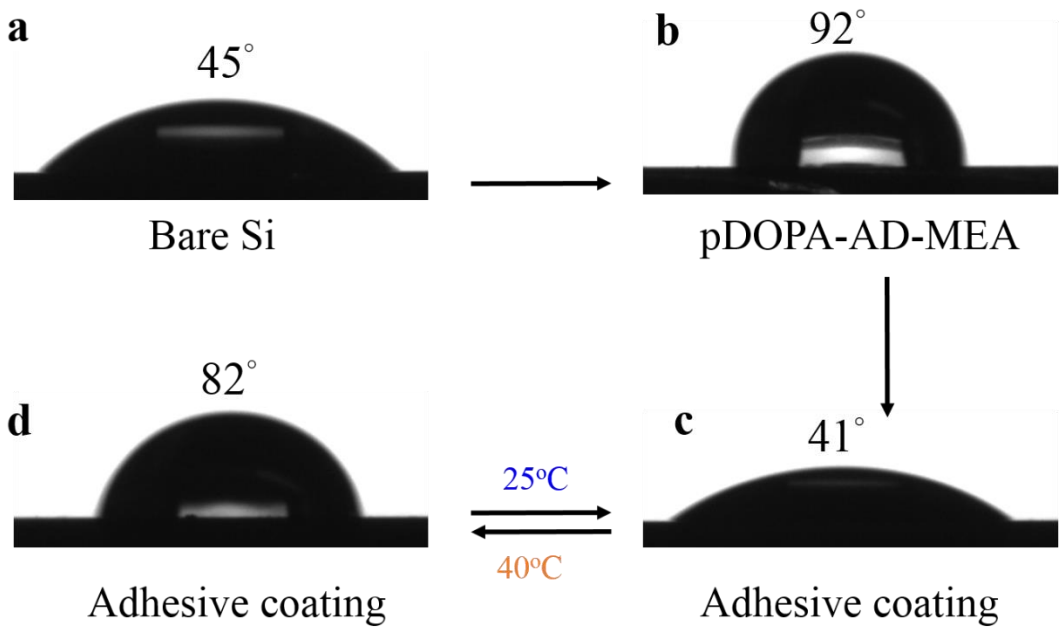


**Supplementary Figure 12 | Contact angle (CA) measurement**. (**a**) A thoroughly cleaned silicon substrate exhibits a hydrophilic property with a water CA of 45°. (**b**) The water CA is increased to 92° after the deposition of the pDOPA-AD-MEA on the silicon substrate due to the existence of hydrophobic MEA monomer in the guest copolymer. (**c**) After the self-assembly of pNIPAM-CD, the water CA at 25°C is reduced to 41°. (**d**) At 40°C, the adhesive surface becomes hydrophobic with a CA of 82° due to the collapse of pNIPAM side-chains.

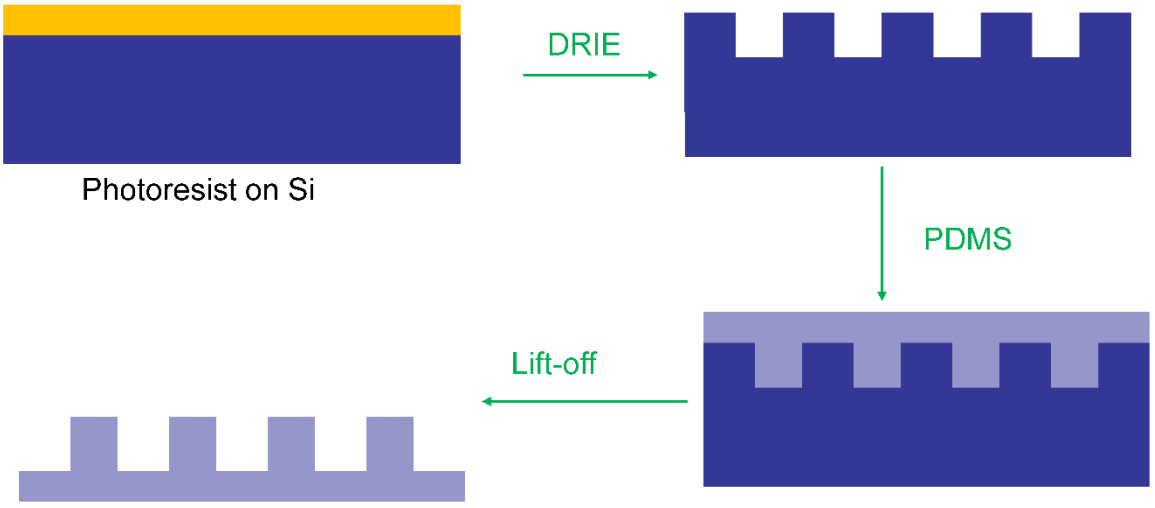


**Supplementary Figure 13 |** Schematic diagram showing the detailed process to fabricate PDMS pillar arrays. A silicon template with micro-hole arrays was first fabricated using photolithography and dry etching. Then PDMS was cast onto the as-fabricated template, followed by curing and lift-off.

**Supplementary Table 1. Element content analysis of bare silicon, pDOPA-AD-MEA, and adhesive coating**

| **Element content (%)** | **C** | **O** | **N** |
|---|---|---|---|
| **Bare Si** | 31.41 | 68.59 | 0 |
| **pDOPA-AD-MEA** | 72.63 | 27.04 | 0.89 |
| **Adhesive coating** | 71.63 | 24.04 | 3.89 |